RSC Advances

ROYAL SOCIETY OF CHEMISTRY

www.rsc.org/advances

Pyridoxal derivative functionalized gold nanoparticles for colorimetric determination of zinc(II) and aluminium(III)

Shilpa Bothra, Rajender Kumar and Suban K Sahoo*

Department of Applied Chemistry, SV National Institute of Technology (SVNIT), Surat-395007, India.

Abstract

This investigation presents the synthesis of a thiol derivative **L** by one step condensation of pyridoxal with 4-aminothiophenol, and its functionalization on citrate capped AuNPs. The nano-assembly **L**-AuNPs was applied for the colorimetric detection of metal ions in aqueous medium. The red color of the **L**-AuNPs solution turns to blue upon addition of Al^{3+} and Zn^{2+} due to the aggregation of nanoparticles. With a high specificity, this nanoprobe detects Al^{3+} and Zn^{2+} with the detection limit down to 0.51 μM and 0.74 μM, respectively. This nano-assembly was also applied for real water sample analysis and construction of INHIBIT logic gate with the two chemical inputs Zn^{2+} and F^-.

*Corresponding author (Dr SK Sahoo): E-mail:suban_sahoo@rediffmail.com; Mob: +91-261-2201814.

Introduction

Research on recognition, sensing and extraction of cations of biological importance have keenly attracted scientists, including chemists, biologists, clinical biochemists and environmentalists. Many alkaline, alkaline-earth and transition metal ions are essentially required for both plants and animals at appropriate concentrations, but show toxicity at relatively high concentrations and threaten to human health through cellular toxicity, liver damage, and neurodegenerative diseases and so on.[1-3] Aluminium, the third most abundant element in the earth's crust is non-essential and toxic to human health.[3] Excessive use of Al^{3+} in food additives, aluminium based pharmaceuticals and storage/cooking utensils has become a causative factor of Parkinson's disease (PD), Alzheimer's disease (AD), dialysis encephalopathy and breast cancer.[4-6] However, till date, the exact mechanisms of Al^{3+} toxicity still remains an open question for study. So, there is a crucial need to track Al^{3+} levels in living cells or other real samples for elucidating its complex physiological and pathological roles. In contrast, Zinc is the essential trace element widely required in cellular functions.[7] Zinc also acts as an intracellular signalling molecule, capable of communicating between cells, converting extracellular stimuli to intracellular signals, and controlling intracellular events. However, abnormal zinc homeostasis causes a variety of health problems that include growth retardation, immune-deficiency, hypogonadism, and neuronal and sensory dysfunctions.[8] Therefore, selective recognition and sensing of the biologically relevant, but spectroscopically silent metal ions, *i.e.* Al^{3+} and Zn^{2+} have been an especially active research area as well as challenging. Various analytical methods such as atomic absorption spectrometry (AAS) [9], inductively coupled plasma atomic emission spectrometry (ICP-AES) [10], ICP mass spectrometry (ICP-MS) [11], electrochemical methods [12] and fluorescent analysis [13] are employed for the detection of Al^{3+} and Zn^{2+} ions. These methods are costly and required sophisticated instruments, and hence demands for developing simple,

sensitive, selective and inexpensive method for rapid and reliable detection of these metal ions in the real environmental samples.

Noble metal nanoparticles such as gold and silver have received great attention in the recent years for the development of colorimetric sensors for the selective detection of various neutral and charged analytes due to their distinctive physical and optical properties such as surface enhanced Raman scattering (SERS) and surface plasmon resonance (SPR). [14-20] Gold nanoparticles (AuNPs) are of particular interest due to their excellent biocompatibility, conductivity and high surface-to-volume ratio, which helps in environmental monitoring and biological sensing.[21-22] AuNPs are widely used in electroanalysis,[21] biosensors,[22] and colorimetric detection[23] and so on. The colorimetric detection of target analytes with AuNPs can be monitored with the color change occurred from red to purple/blue due to the aggregation or the corrosion of AuNPs.[23-26] Literature survey revealed that very few colorimetric methods for the detection of Al^{3+} and Zn^{2+} are reported using surface functionalized AuNPs, in compared to other metal ions such as Hg^{2+}, Cu^{2+}, Pb^{2+} etc.[27-35] Also, the nanoprobes have been recently applied for the construction of Boolean logic gates, which are promising in the fabrication of molecular computation and becoming a potential substitute for the traditional silicon-based computation.[36-41]

Continuing our research on the chemosensors development with vitamin B_6 cofactors like pyridoxal (PL), pyridoxal 5-phosphate (PLP),[42-44] herein, we have developed a rapid colorimetric nanoprobe with good selectivity for Al^{3+} and Zn^{2+} using an organic ligand functionalized AuNPs. The ligand **L** was synthesized by reacting pyridoxal with an equimolar amount of 4-aminothiophenol (Fig. 1) and coated over the surface of the AuNPs by the ligand exchange method. Then, the **L**-AuNPs system was applied for the colorimetric sensing of metal ions. The complexation induced decrease in the inter-nanoparticles distance triggered the aggregation of **L**-AuNPs which allowed the selective detection of Al^{3+} and Zn^{2+}

with a distinct color change from red to blue and appearance of a red shifted SPR band at 650 nm.

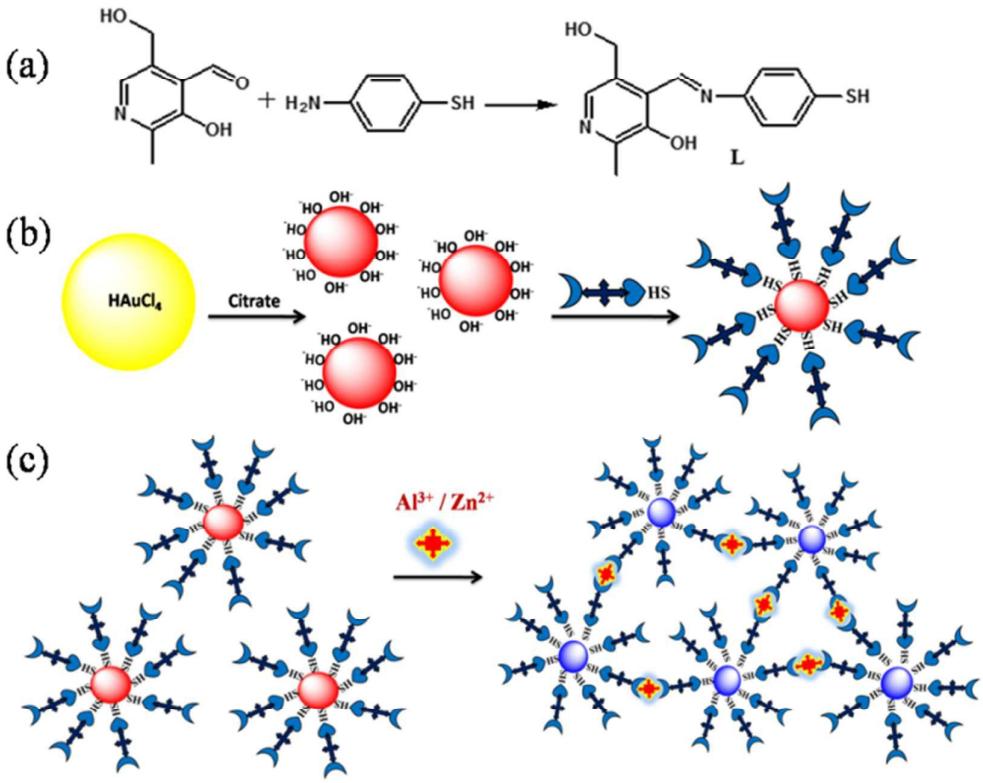

Fig. 1. Schematic representation for (a) the synthesis of ligand **L** and (b) its functionalization over AuNPs surface, and (c) the complexation induced aggregation of **L**-AuNPs.

Experimental

Materials and instrumentations

All the starting reagents used for the experiments were purchased commercially in the purest form and were used without further purification. $HAuCl_4.3H_2O$ was purchased from Sigma Aldrich, India. Sodium citrate trihydrate was purchased from Finar Pvt. Ltd., India. All the metal salts used for the experiments were purchased from Rankem Pvt. Ltd., India and inorganic anions were used in form of Na/K salts such as Sodium Fluoride (NaF), potassium

iodide (KI), potassium bromide (KBr), sodium chloride (NaCl), sodium acetate (NaAcO), and sodium phosphate ($NaH_2PO_4.2H_2O$).

All glasswares were cleaned with a diluted HNO_3 solution and rinsed with Milli-Q water prior to use. Stock solutions of the metal ions (1 x 10^{-2} M and 1 x 10^{-3} M) and inorganic anions (1 x 10^{-3} M) were prepared freshly in Milli-Q water. These solutions were used for all spectroscopic studies after appropriate dilution. Hydrochloric acid (0.1 N) and sodium hydroxide (0.1 N) solutions were used to adjust the pH.

The UV-Vis absorption spectra were recorded in aqueous medium on a Cary 50 Varian UV-Vis spectrophotometer at room temperature using quartz cells with 1.0 cm path length in the range of 200–800 nm. The observed pH was measured as -log (H^+) using a HANNA HI 2223 pH meter equipped with a calibrated combined glass electrode with standard buffer solutions. FT-IR spectra were recorded on a FTIR spectrophotometer DRS (8400-S-Shimadzu) using KBr pellet. Elemental analysis was measured by using the CE Instrument Corporation EA 1108. Transmission electron microscopy (TEM) was recorded on a Philips CM 200 transmission electron microscope operated at an accelerating voltage 200 kV. For TEM analysis, the samples were prepared by drop-coating AuNPs dispersions onto carbon-coated copper TEM grids, which were subsequently air-dried. The DLS data were obtained using Malvern Zeta size Nano (Malvern, UK).

Synthesis of L

Pyridoxal hydrochloride (200 mg, 0. 98 mmol) was treated with 4-aminothiophenol (122.6 mg, 0. 98 mmol) in methanol (20 mL) and the mixture was stirred for 30 minutes. The red colored precipitates were collected, washed with cold ethanol and then dried. Yield: 76%, FTIR (KBr pellet, cm^{-1}): 3202, 3040, 2639, 2556, 2463, 1615, 1560, 1485, 1306, 1209, 1042, 999, 882, 841, 687, 571, 500, 444; ^{1}H NMR (DMSO-d_6, 400 MHz, ppm): δ 2.51 (CH_3, s), 3.61 (-SH, b), 4.89(-CH_2-, s), 5.10 (-OH, s), 7.30 (Ar-N, d), 6.81 (Ar-H, d), 7.69 (Ar-H, s),

8.30 (Ar-H, s), 8.33 (-CH=N-, s), 11.65 (-OH, b); Anal. Calcd for $C_{14}H_{15}ClN_2O_2S$: C, 54.10; H, 4.86: N, 9.01. Found: C, 53.98; H, 4.87: N, 9.17.

Synthesis of bare and L functionalized AuNPs

Bare gold nanoparticles (AuNPs) were synthesized by the citrate-mediated reduction of $HAuCl_4$ according to the published protocol with necessary modifications.[45] Briefly, an aqueous solution of $HAuCl_4$ (50 ml, 1 x 10^{-3} M) was heated to reflux with vigorous stirring in a round-bottom flask fitted with a reflux condenser and then sodium citrate (5 ml, 38.8 x 10^{-3} M) was rapidly added to the boiled solution. The mixed solution was boiled for another 30 min to produce wine red AuNPs. The obtained solution was cooled to room temperature and stored at 4°C. These AuNPs were very stable owing to the electrostatic repulsion invoked by citrate ligand adsorbed on the particles surface.

The functionalized AuNPs were prepared at room temperature by drop wise addition of 0.5 ml of synthesized capping agent **L** in ethanol (1 x 10^{-5}M) to 10 ml of the above gold colloids, where **L** molecules were adsorbed on the AuNPs surface through ligand-exchange reaction. The reaction mixture was stirred for approximately 2 h to ascertain the self-assembly capping agent on the AuNPs surface. The functionalized AuNPs were kept at 4°C for further use.

Colorimetric detection of metal ions using L-AuNPs

The prepared **L**-AuNPs were diluted further with water in 1:2 (v/v) and then required amount was taken for different experiments. For colorimetric detection, many tests were carried out to optimize the sensing conditions for metal ions by adding different concentrations of metal ions to the prepared **L**-AuNPs and to check the instant colorimetric changes. For the selectivity study, 1 ml of metal ion (1 x 10^{-3}M) was added into 1 ml of functionalized AuNPs (2.14 nM).[46] For spectrophotometric titrations, required amount of the AuNPs was taken directly into quartz cuvette and then the spectra were recorded after each

aliquot addition of metal ions ((Al^{3+}) and (Zn^{2+}) = 1.0 x 10^{-2} M) using micropipette. The change in the SPR band was plotted against metal ion concentrations to obtain different analytically useful data. For real sample analyses, tap water was directly spiked with standard Al^{3+} and Zn^{2+} solutions to different concentrations. These spiked samples were then analyzed separately using the developed calibration curve.

Results and discussion

Synthesis and functionalization of AuNPs

The ligand **L** was synthesized by direct condensation of pyridoxal with 4-aminothiophenol in methanol (Fig. 1). The citrate capped AuNPs were synthesized by reduction of $HAuCl_4$ solution and characterized by UV-Vis spectroscopy that showed the characteristic SPR band at 525 nm (Fig. 1S). The ligand **L** was coated on the AuNPs surface by ligand-exchange method. The higher affinity of thiol group of **L** is preferentially linked to the AuNPs surface to form the **L** coated AuNPs *i.e.* **L**-AuNPs. Analysis by TEM indicates the formation of spherical shaped **L**-AuNPs of size ca. 15±2 nm (Fig. 2a) that dispersed well in the solution was supported by the DLS measurement (Fig. 2S).

The effect of pH was investigated on the colloidal stability of **L**-AuNPs in aqueous solution by using the UV−Vis absorption spectroscopy (Fig. 3S). The solutions with the desired pH values were prepared by adding 0.1 N HCl or 0.1 N NaOH. The **L**-AuNPs solutions were found to be stable in the pH range of 4.0 to 10.0. Lowering of pH less than 4.0, the particles aggregated showing color change from red to purple to blue, which is also supported by UV-Vis spectrum from the red shift in the SPR band from 525 nm to 650 nm at pH 2.0.

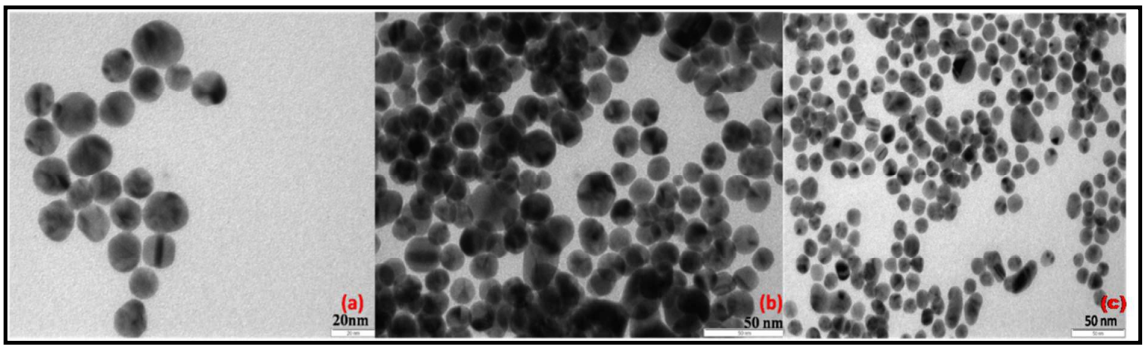

Fig. 2. TEM images of **L**-AuNPs in absence (a) and presence of (b) Al^{3+} and (c) Zn^{2+}.

Colorimetric sensing of metal ions using L-AuNPs

The applications of the sensitivity of the position of the SPR band of gold nanoparticles are well known especially in the fields of sensors and biology. The visual sensing ability of gold nanoparticles relies on the color change arising from the SPR phenomenon mainly through analyte triggered aggregation of nanoparticles.[47] The response of **L**-AuNPs was examined over a series of metal ions, such as Fe^{2+}, Fe^{3+}, Mn^{2+}, Co^{2+}, Ni^{2+}, Cu^{2+}, Zn^{2+}, Pb^{2+}, Mg^{2+}, Al^{3+}, and Hg^{2+} (Fig. 3). Addition of Al^{3+} and Zn^{2+} to **L**-AuNPs solution results in an instantaneous color change from red to blue and the SPR band at 525 nm was red-shifted to ~650 nm. No obvious color or spectral changes were observed with other tested metal ions. As explained in Fig. 1 and supported with TEM analysis of **L**-AuNPs solution containing Al^{3+} (Fig. 2b) and Zn^{2+} (Fig. 2c), the aggregation of nanoparticles was occurred due to the selective complexation of metal ions with the coated ligand **L**. Comparison of the FT-IR of **L**-AuNPs alone and in the presence of Al^{3+} and Zn^{2+} indicates the possible complexation occurred through the imine-N and pyridoxal-OH of capped **L** (Fig. 4S). The characteristic C=N stretching vibrational band of **L** at 1615 cm^{-1} in **L**-AuNPs was shifted to 1623 cm^{-1} and 1653 cm^{-1} respectively in the presence of Al^{3+} and Zn^{2+}, and the –OH bending vibration of **L**-AuNPs at 1264 cm^{-1} was disappeared. Further analysis by DLS measurement confirmed that the average size of **L**-AuNPs increased drastically to 213 nm

upon addition of Al^{3+} due to the aggregation of nanoparticles (Fig. 2S). In addition, the selectivity of **L**-AuNPs was also analyzed by adding different anions such as F^-, Cl^-, Br^-, I^-, $H_2PO_4^-$ and AcO^-. No noticeable changes in the color and SPR band of **L**-AuNPs were observed in the presence of different anions (Fig. 5S).

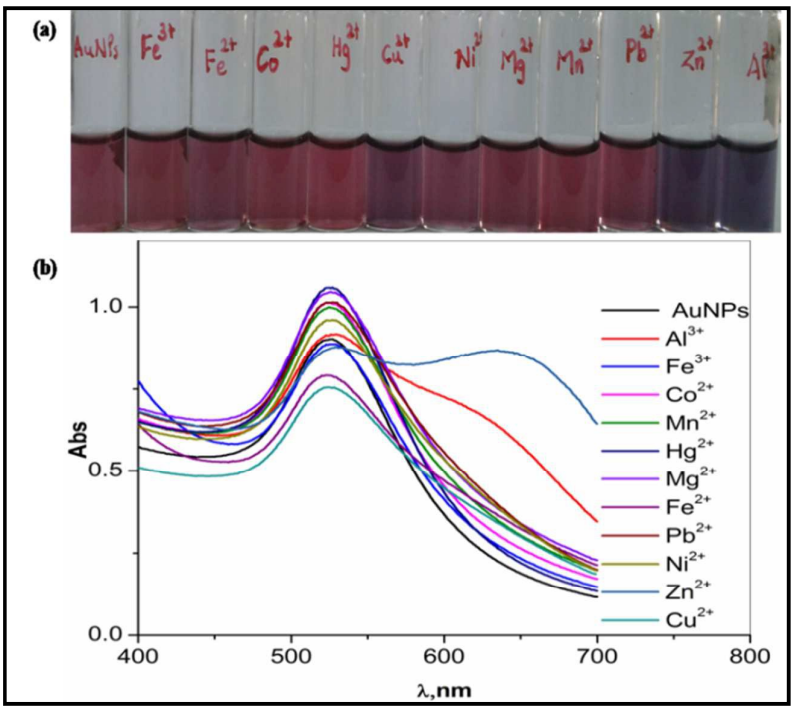

Fig. 3 (a) Colorimetric and (b) UV-Vis spectral changes of **L**-AuNPs in the presence of different metal ions (5.0×10^{-4} M).

The analytical applicability of **L**-AuNPs to detect Al^{3+} and Zn^{2+} was examined by performing the competitive experiments (Fig. 6S). For these competitive experiments, the color and spectral changes of **L**-AuNPs in the presence of Al^{3+}/Zn^{2+} was investigated in the presence of equimolar amount of other interfering metal ions. No obvious interference was seen when Al^{3+}/Zn^{2+} (2.5×10^{-4}M) was added to an aqueous solution of **L**-AuNPs suggesting that this nano-assembly can be used to specifically determine Al^{3+} and Zn^{2+} by colorimetric method.

The spectrophotometric titrations of **L**-AuNPs were performed with incremental addition of Al^{3+} (Fig. 4a) and Zn^{2+} (Fig. 5a) to determine the detection limit. Upon successive

addition of Al^{3+} and Zn^{2+} to a fixed concentration of **L**-AuNPs resulted gradual broadening and decrease in the intensity of the SPR band at 525 nm along with the appearance of a new band at ~650 nm. Addition of Al^{3+} and Zn^{2+} to the system resulted a significant color change from a wine red to purple and finally to blue. This can be easily judged visually, even when the concentration is as low as 1.96 x 10^{-5} M for Al^{3+} and 2.59 x 10^{-5} M for Zn^{2+}. The spectral responses of **L**-AuNPs were found linearly proportional to the concentrations of Al^{3+} between 6.62 x 10^{-5} M to 3.22 x 10^{-4} M (Fig. 4b) and for Zn^{2+} between 6.62 x 10^{-5} M to 4.45 x 10^{-4} M (Fig. 5b). The detection limit was determined from three times the standard deviation of the blank signal (3σ/slope) as 0.51 μM for Al^{3+} and 0.74 μM for Zn^{2+}. The estimated detection limit for Al^{3+} and Zn^{2+} was far better than the acceptable limit of 1.85 μM Al^{3+} and 76 μM Zn^{2+} suggested respectively by the US-EPA and World Health Organization (WHO) for drinking water.[48,49]

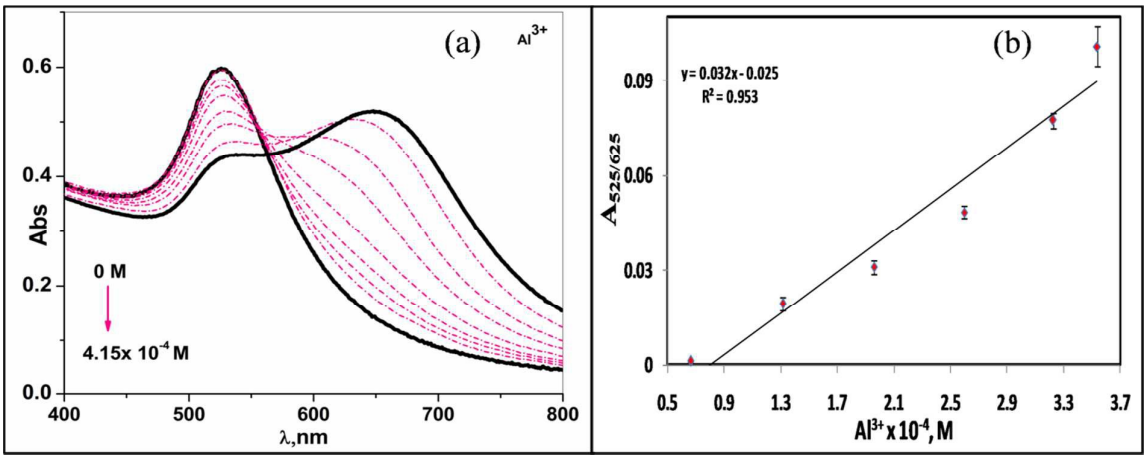

Fig. 4. (a) UV-Vis spectral changes of **L**-AuNPs at various concentrations of Al^{3+} (0 to 4.15 x 10^{-4} M) and (b) calibration curves for quantification Al^{3+} using **L**-AuNPs.

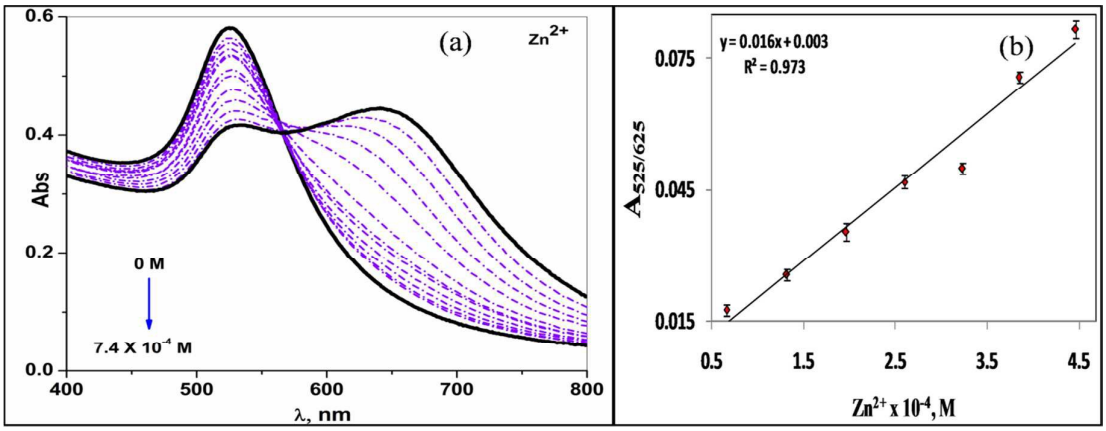

Fig. 5. (a) UV-Vis spectral changes of **L**-AuNPs at various concentrations of Zn^{2+} (0 to 7.40 x 10^{-4} M) and (b) calibration curves for quantification Zn^{2+} using **L**-AuNPs.

To investigate the practical applications of this colorimetric method, the detection of Al^{3+} and Zn^{2+} in real water samples was carried out by using the **L**-AuNPs. After addition of the spiked water sample into the **L**-AuNPs solution, the UV-Vis spectra of the samples were recorded. As summarized in Table 1S, the **L**-AuNPs showed good recovery percentage which clearly supported the analytical potential in real samples analysis. Further, the importance of **L**-AuNPs nanosensing system was checked by comparing the analytical parameters with the reported AuNPs based sensors (Table 2S and Table 3S). [27-35] This nanosystem showed comparable analytical performance for the detection of Al^{3+} and Zn^{2+} with the reported AuNPs based colorimetric assay and can be applied over a wide pH range.

Finally, the optical response of **L**-AuNPs was tested in the presence of F^- and the two selective metal ions Al^{3+} and Zn^{2+}. Addition of F^- caused a reversal of the **L**-AuNPs aggregation induced by Zn^{2+} but not in the presence of Al^{3+}. These results encourage us to construct a logic gate by using F^- and Zn^{2+} as chemical inputs, and the color change of **L**-AuNPs as outputs. The absence and presence of each input are defined as "0" and "1", respectively. The well-dispersed red **L**-AuNPs solution is defined as output "0", and the blue solution containing aggregated AuNPs as output "1". In the (0, 0) state, **L**-AuNPs solution was red and well dispersed. Addition of Zn^{2+}, *i.e.* (0, 1) state induced aggregation. However,

in the (1, 0) and (1, 1) state, when F^- alone or both F^- and Zn^{2+} was introduced into the **L**-AuNPs solution, no aggregation of AuNPs can be observed. As depicted in Fig. 6, the optical changes of **L**-AuNPs mimic the INHIBIT logic gate (a combination of AND and NOT logic gates).

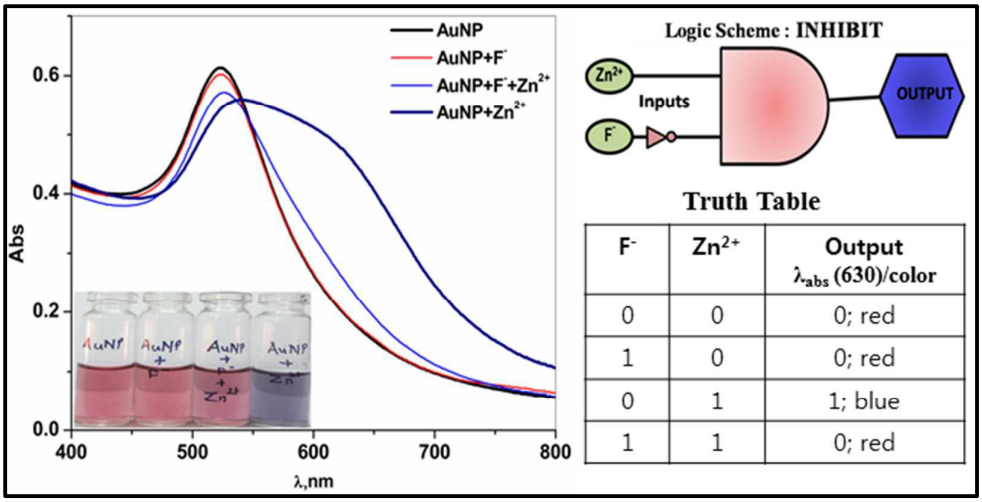

Fig. 6. Operation of the INHIBIT logic gate. Left: the UV-Vis spectral and color changes of **L**-AuNPs with the two inputs (Zn^{2+} and F^-). Right: the logic scheme and truth table.

Conclusions

In conclusion, we have introduced a nano-assembly **L**-AuNPs for the selective colorimetric detection of Al^{3+} and Zn^{2+} in aqueous medium. This **L**-AuNPs system was not only simple but also rapid, sensitive and selective for the detection of Al^{3+} and Zn^{2+} over the other tested metal ions. The estimated detection limit was found to be far better than the permissible limit for Al^{3+} and Zn^{2+} in drinking water. Also, this sensor was successfully applied for the detection of Al^{3+} and Zn^{2+} in real water samples.

Acknowledgments

This work was made possible by a grant from the DST, New Delhi (SR/S1/IC-54/2012). We would also like to thank SAIF, Indian Institute of Technology (IIT), Bombay for providing TEM facility.

References

1. S.K. Sahoo, D. Sharma, R.K. Bera, G. Crisponi and J.F. Callan, *Chem. Soc. Rev.*, 2012, **41**, 7195.
2. G. R. C. Hamilton, S.K. Sahoo, S. Kamila, N. Singh, N. Kaur, B.W. Hyland and J.F. Callan, *Chem. Soc. Rev.*, 2015, **44**, 4415.
3. M. Baral, S.K. Sahoo and B.K. Kanungo, *J. Inorg. Biochem.*, 2008, **102**, 1581.
4. M. Yasui, T. Kihira and K. Ota, *Neurotoxicol.*, 1992, **13**, 593
5. P. D. Darbre, *Eur. J. Cancer Prev.*, 2001, **10**, 389.
6. P. D. Darbre, *J. Appl. Toxicol.*, 2003, **23**, 89.
7. W.G. Telford and P.J. Fraker, *J. Cell Physiol*, 1995,**164**,259.
8. C.J. Frederickson, J.Y. Koh and A.I. Bush, *Nat. Rev. Neurosci.*, 2005, **6**,449.
9. P. Chappuis, J. Poupon and F. Rousselet, *Clin. Chim. Acta*, 1992, **206**, 155.
10. L. J. Melnyk, J. N. Morgan, R. Fernando, E. D. Pellizzari and O. Akinbo, *J. AOAC Int.*, 2003, **86**, 439.
11. H. M. Wang, Z. L. Yu, Z. L. Wang, H. J. Hao, Y. M. Chen and P. Y. Wan, *Electroanal.*, 2011, **23**, 1095.
12. X. J. Xie and Y. Qin, *Sens. Actuators,* B, 2011, **156**, 213.
13. B. Wiley, Y. Sun and Y. Xia, *Acc. Chem. Res.*, 2007, **40**, 1067.
14. P.K. Sudeep, S.T.S. Joseph and K.G. Thomas, *J. Am. Chem. Soc.*, 2005, **127**, 6516.
15. J.W. Xin, F.Q. Zhang and Y.X. Gao, et al., *Talanta*, 2012,**101**, 122.
16. K.A. Willets, *Anal. Bio-Anal. Chem.*, 2009, **394**, 85.
17. M.D. Porter, R.J. Lipert and L.M. Siperko, et al., *Chem. Soc. Rev.*, 2008, **37**, 1001.
18. P.K. Jain, K.S. Lee and I.H. El-Sayed, et al., *J. Phys Chem. B*., 2006, **110**, 7238.
19. H.W. Huang, X.Y. Liu and T. Hu, et al., *Biosens. Bioelectron.*, 2010, **25**, 2078.
20. C.A. Mirkin, R.L. Letsinger and R.C. Mucic, et al., *Nat.*, 1996, **382**, 607.

21. Y. Y. Li, H. J. Schluesener and S. Q. Xu, *Gold Bull.*, 2010, **43**, 29.

22. M. Zhang, Y. Q. Liu and B. C. Ye, *Chem. Comm.*, 2011, **47**, 11849.

23. J. R. Kalluri, T. Arbneshi, S. A. Khan, A. Neely, P. Candice, B. Varisli, M. Washington, S. McAfee, B. Robinson, S. Banerjee, A. K. Singh, D. Senapati and P. C. Ray, *Angew. Chem.*, 2009, **121**, 9848.

24. Y. M. Fang, J. Song, J. S. Chen, S. B. Li, L. Zhang and G. N. Chen, J. J. Sun, *J. Mater. Chem*., 2011, **21**, 7898.

25. J. J. Storhoff, A. A. Lazarides, R. Mucic, C. A. Mirkin, R. Letsinger and G. C. Schatz, *J. Am. Chem. Soc.*, 2000, **122**, 4640.

26. C. A. Mirkin and J. J. Storhoff, *Chem. Rev.*, 1999, **99,** 1849.

27. S. Chen, Y.M. Fang, Q. Xiao, J. Li, S. B. Li, H. J. Chen, J. J. Sun and H. H. Yang, *Analyst*, 2012, **137**, 2021.

28. X. Li, J. Wang, L. Sun and Z. Wang, *Chem. Commun.*, 2010, **46**, 988.

29. M. Zhang, Y. Q. Liu and B.C. Ye, *Chem. Eur J.*, 2012, **18**, 2507.

30. Y. C. Chen, I. L. Lee, Y. M. Sung and S. P. Wu, *Talanta*, 2013, **117**, 70.

31. S. Promnimit, T.Bera, S. Baruah and J. Dutta, *J. Nano Res*., 2011, **16**, 55.

32. E.M.S. Azzam, A.F.M. El- Farargy and A. A. Abd-Elaal, *J. Ind. Eng. Chem.,* 2014, **20** 3905.

33. R. Selegård, K. Enander and D. Aili, *Nanoscale*, 2014, **6**, 14204.

34. W. Li, Z. Nie, K. He, X. Xu, Yong Li, Y. Huang and S. Yao, *Chem. Commun.,* 2011, **47**, 4412.

35. S. H. Jung, S. H. Jung, J. H. Lee, M. Je and M. Y. Choi, *Bull. Korean Chem. Soc.*, 2015, **36**, 2408.

36. U. Pischel, *Angew. Chem. Int. Ed.*, 2007, **46**, 4206.

37. A. Prokup, J. Hemphill and A. Deiters, *J. Am. Chem. Soc.*, 2012, **134**, 3810.

38. J. Elbaz, O. Lioubashevski, F. Wang, F. Remacle, R. D. Levine and I. Willner, *Nat. Nanotechnol.*, 2010, **5**, 417.

39. T. Li, E. Wang and S. Dong, *J. Am. Chem. Soc.*, 2009, **131**, 15082.

40. K. Szacilowski, *Chem. Rev.*, 2008, **108**, 3481.

41. D. Sharma, A. Moirangthem, R. Kumar, S. K. Ashok Kumar, A. Kuwar, J. F. Callan, A. Basu and S. K. Sahoo, *RSC Adv.*, 2015, **5**, 50741.

42. D. Sharma, S. K. Ashok Kumar and S. K. Sahoo, *Tetrahedron Lett.*, 2014, **55**, 927.

43. D. Sharma, S. K. Sahoo, S. Chaudhary, R. K. Bera and J. F. Callan, *Analyst*, 2013, **138**, 3646.

44. W. Haiss, N. Thanh, J. Aveyard, D. Fernig, *Anal. Chem.*, 2007, **79**, 4215.

45. J.T.K.M.M. Alvarez, T.G. Schaaff, M.N. Shafigullin, I. Vezmar, R.L. Whetten, *J. Phys. Chem. B*, 1997, **101**, 3706.

46. S. Wang, X. Wang, Z. Zhang, L. Chen, *Colloid Surface A,* 2015, **468**, 333.

47. J.T.K.M.M. Alvarez, T.G. Schaaff, M.N. Shafigullin, I. Vezmar, R.L. Whetten, *J. Phys. Chem. B*, 1997, **101**, 3706.

48. J. Hatai, M. Samanta, V. S. R. Krishna, S. Pal and S. Bandyopadhyay, *RSC Adv.*, 2013, **3**, 22572.

49. A. Hens, A. Maity, K. K. Rajak, *Inorg. Chim. Acta*, 2014, **423**, 408.